Key Engineering Materials
ISSN: 1662-9795, Vol. 984, pp 71-76
doi:10.4028/p-P2s0sP

Submitted: 2023-09-30
Accepted: 2024-02-04
Online: 2024-08-22

Experimental Observation of Raman Assisted and Kerr Optical Frequency Comb in a 4H-Silicon-Carbide on Insulator Microresonator

Adnan Ali Afridi[1,a*], Yaoqin Lu[1,b], Xiadong Shi[1,c], Ruixuan Wang[2,d], Jingwei Li[2,e], Qing Li[2,f], and Haiyan Ou[1,g]

[1]Department of Electrical and Photonics Engineering, Technical University of Denmark (DTU), Kongens Lyngby, 2800, Denmark

[2]Department of Electrical and Computer Engineering, Carnegie Mellon University, Pittsburgh, Pennsylvania 15213, USA

[a]aalaf@dtu.dk, [b]yaolu@dtu.dk, [c]xshi@fotonik.dtu.dk, [d]ruixuanw@andrew.cmu.edu, [e]jingwei5@andrew.cmu.edu, [f]qingli2@andrew.cmu.edu, [g]haou@dtu.dk

Keywords: Silicon Carbide, Microresonator, Raman Comb, Four Wave Mixing, Kerr Optical Frequency Comb

Abstract. Kerr nonlinear microcavities have garnered significant interest owing to their rich dynamics of nonlinear optical phenomena and compatibility with on-chip photonic integration. Recently, silicon carbide has emerged as a compelling platform due to its unique optical properties. In this study, we demonstrate Raman-assisted and Kerr optical frequency generation in a 4H-silicon carbide-on-insulator microresonator. By pumping the transverse electric (TE_{00}) mode within the device, we observe a stimulated Raman scattering (SRS) Stokes with the Raman shift at approximately 775 cm^{-1}, achieved with an on-chip power of 350 mW. Furthermore, by red-tuning the TE_{00} pump wavelength, we have achieved the coexistence of Raman and Kerr frequency combs. Using another device on the same chip with light variation of the taper we can observe the Raman and Kerr frequency combs within a spectral bandwidth ranging from $\sim$ 1440 to 1960 nm. The inclusion of the Raman-assisted comb extends the comb's coverage into longer wavelength regimes, making it highly desirable for spectroscopy applications.

Introduction

High-Q Kerr nonlinear optical microcavities have revolutionized the field of optical frequency comb technology. Over the past decade, the development of frequency comb technology has significantly attracted research interests due to its potential in out-of-lab commercial applications [1]. To date, frequency combs have played a pivotal role in various applications, such as communication [2], LiDAR [3], frequency synthesizer [4] and dual-comb spectroscopy [5], etc. Furthermore, the demand for broadband frequency combs with low power consumption and minimal noise are the fundamental requirements for the photonics integration and led to the exploration of various material platforms, including silica [6], silicon (Si) [7], silicon nitride (Si_3N_4) [8,9], aluminium nitride (AlN) [10,11,12], lithium niobate ($LiNbO_3$) [13], aluminium gallium arsenide (AlGaAs) [14], and silicon carbide (SiC) [15,16,17].

SiC material has recently emerged as a highly promising material platform for photonics and nonlinear optics, owing to its exceptional optical and nonlinear properties. SiC boasts a wide bandgap ranging from 2.2 eV to 3.4 eV, which, coupled with its low two-photon absorption (TPA), imparts unique advantages. Additionally, it exhibits high thermal conductivity, a broad transparency window encompassing the visible to mid-infrared regions, and a high refractive index of 2.6 at telecom wavelengths, allowing for robust light confinement [17]. What sets SiC apart is its dual nonlinear behavior, featuring both strong third-order (χ^3) and second-order (χ^2) nonlinearities [18], making it a significant platform not only for optical applications but also for metrology applications [19], where its properties find diverse and critical utility. Moreover, among other polytypes of SiC, 4H-SiC has showcased an exceptionally high-quality factor (Q) [16, 20], establishing its efficacy in generating frequency combs with efficiency [16]. Here we report, the generation of Raman comb and Kerr frequency comb in 4H-SiC-on-insulator microresonator.

Results

Device design and Simulation. We employ a 4H-SiC-on-insulator microresonator with a free spectral range (FSR) of around 474 GHz and cross-section of 1×0.63 μm^2 (width×thickness), shown in the schematic of Fig. 1(a). The fully-etched device was made of Cree 4H-SiCOI and fabricated using a similar process as discussed in Ref. [16]. The waveguide of 4H-SiCOI is embedded in silicon dioxide (SiO_2) and inverse tapers were successfully implemented by polishing the two facets of SiC, achieving a total insertion loss <12 dB. Microscopic image of one of the devices microring cavity is shown in Fig. 1(b). For an efficient four wave mixing (FWM) Kerr comb generation anomalous group velocity dispersion (D>0) is vital [21]. Considering a sidewall angle (θ) of 80^o of the waveguide we simulated eigen frequencies using the finite element modeling (FEM) multiphysics Comsol software. Furthermore, as illustrated in Fig. 1(c), based on the simulated eigen frequencies the group velocity dispersion (GVD) for the TE fundamental and transverse magnetic (TM) fundamental modes are calculated using an equation, e.g.

$$D = -\frac{\lambda}{c}\frac{d^2 n_{eff}}{d\lambda^2} \tag{1}$$

where λ is wavelength, c is the velocity of light and n_{eff} is an effective refractive index. The extracted second-order dispersions D_2 values for TE and TM fundamental polarization modes are around 34

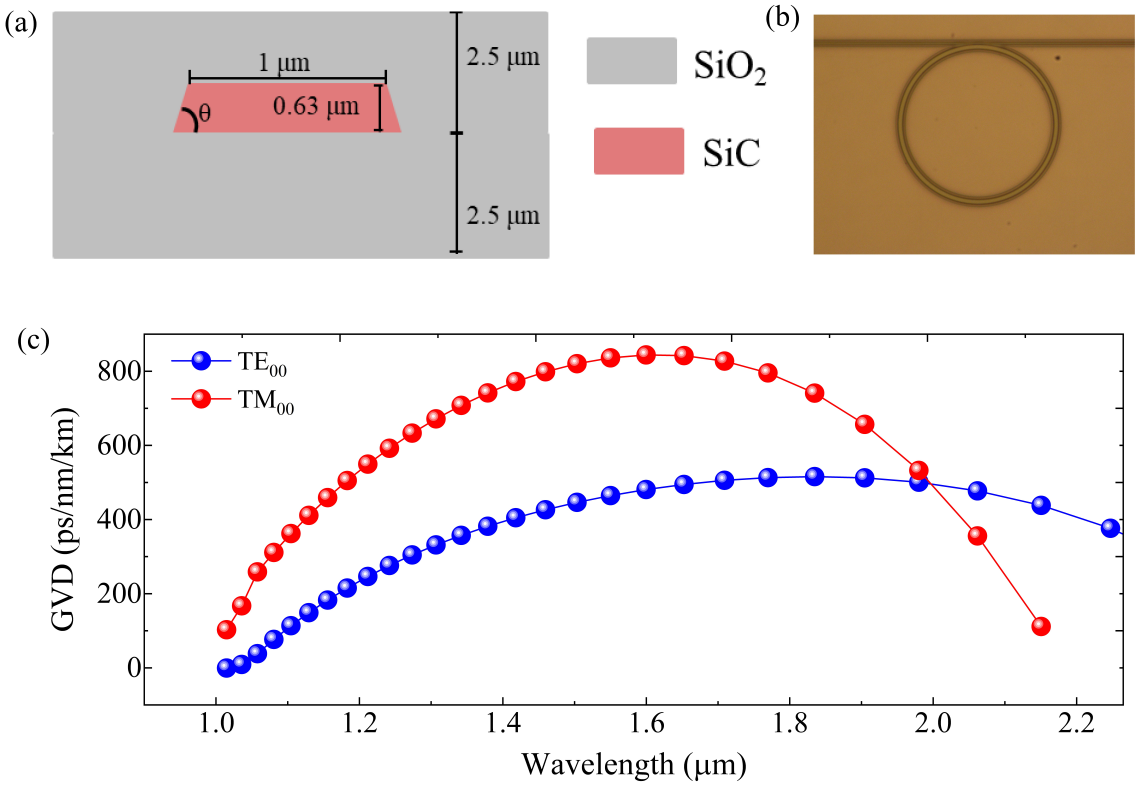

Fig. 1: (a) Schematic diagram of a cross-section of the 0.63 μm thick 4H-SiCOI microresonator having a sidewall angle (θ) of 80^o, embedded in SiO_2. (b) Shows a microscopic image of one of the fabricated microcavities. (c) Simulated group velocity dispersion (GVD) for both the TE_{00} and TM_{00} polarization modes for a 36 μm cavity with the ring width (RW) of 1 μm.

and 57 MHz, respectively. The second-order dispersion D_2 correspond to GVD parameter β_2. The simulated FSRs (using the FEM method) are 477 and 455 GHz for both the TE_{00} and TM_{00} polarization modes and can agree very well to our experimental value.

Experimental Setup. Fig. 2 presents a schematic of an experimental setup necessary for accessing the frequency combs in microresonators [21]. The continous wave (cw) laser pump source utilized in this work is from Santec TSL-510 with a wavelength resolution of 5 pm. The cw laser light is amplified using an erbium-doped amplifier (EDFA) and launched into the 4H-SiCOI microresonator using the lensed fibers to excite the frequency comb. The desired mode of polarization is selected by adjusting the pedals of the fiber polarization controller (FPC). The pump laser wavelength can be tuned into the cavity using the front panel of the laser source. The frequency comb spectrum is collected by another lensed fiber at the output of the waveguide and recorded using a Yokogawa optical spectrum analyzer (OSA). During the experiment, the input and output powers of the system are monitored using a Santec multi-port power meter (MPM).

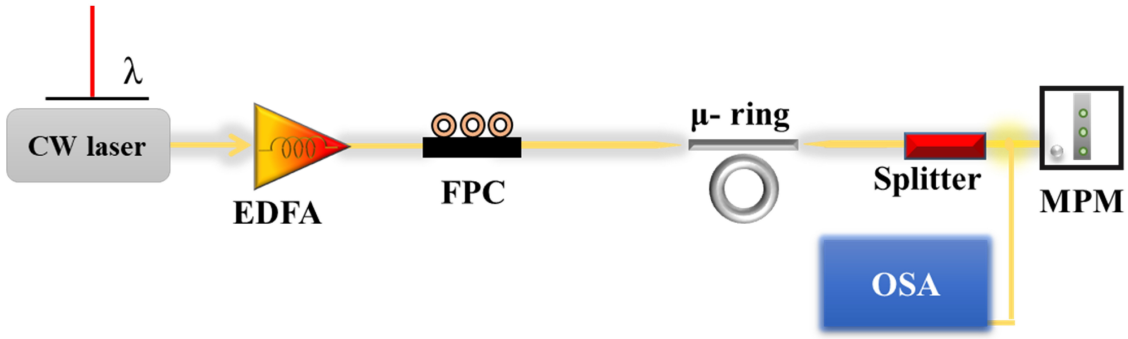

Fig. 2: Schematic setup for the generation of the Raman comb and Kerr optical frequency comb. CW laser: continuous wave laser, EDFA: erbium-doped amplifier, FPC: fiber polarization controller, OSA: optical spectrum analyzer, MPM: multi-port power meter.

Raman and Kerr frequency comb generation. To achieve the frequency comb, we select the desired polarization mode (TE_{00} in our experiment) resonance on the pump source and amplify it using the EDFA. The chip coupling loss is around 6 dB per facet and we set the amplifier's output power relatively high at around 900 mW i.e., 350 mW in the waveguide. We then tune the laser wavelength from the blue to the red position of the pump wavelength ($\sim$1545 nm). The generated spectra are observed and recorded using the optical spectrum analyzer (OSA) and plotted in Fig. 3. From Fig. 3, we observe the first stokes at around 1775 nm and the calculated Raman shift of 775.8 cm-1 which corresponds to the phonon E2(TO) [14,23]. Upon further tuning the pump wavelength, we can access the SRS stokes and different comb states such as, the state I Raman comb with few adjacent sideband lines, in state II new sideband comb lines emerge due to the cascaded process. Furthermore, in the final state III before the cavity is at zero resonance Raman comb together with the Kerr four-wave mixing (FWM) adjacent primary comb lines are generated. Moreover, we employ another microresonator (36 μm radius) on the same chip with a slight variation of the taper bus waveguide. We select the TE_{00} mode near 1566 nm and the normalized resonance is shown in the inset of Fig. 4. The free spectral range (FSR) is around 473 GHz and extracted an intrinsic quality factor of 0.3 million. It is important to note that the lower quality factor compared to the earlier reported results in ref. [16] is attributed to smaller widths. Through forward tuning, wherein the laser wavelength is systematically varied from the blue to the red side, we observe the generation of SRS Stokes, followed by the emergence of the Raman-assisted comb and the Kerr comb. It is worth mentioning that during the frequency comb generation in our 4H-SiCOI platform, the Raman effect is dominant [24, 25, 26]. Finally, a broadband Raman comb together with the Kerr comb having a single FSR is generated in the wavelength range of around 1450 to 1900 nm of around 1450 to 1900 nm. The recorded spectrum is shown in Fig. 4, respectively.

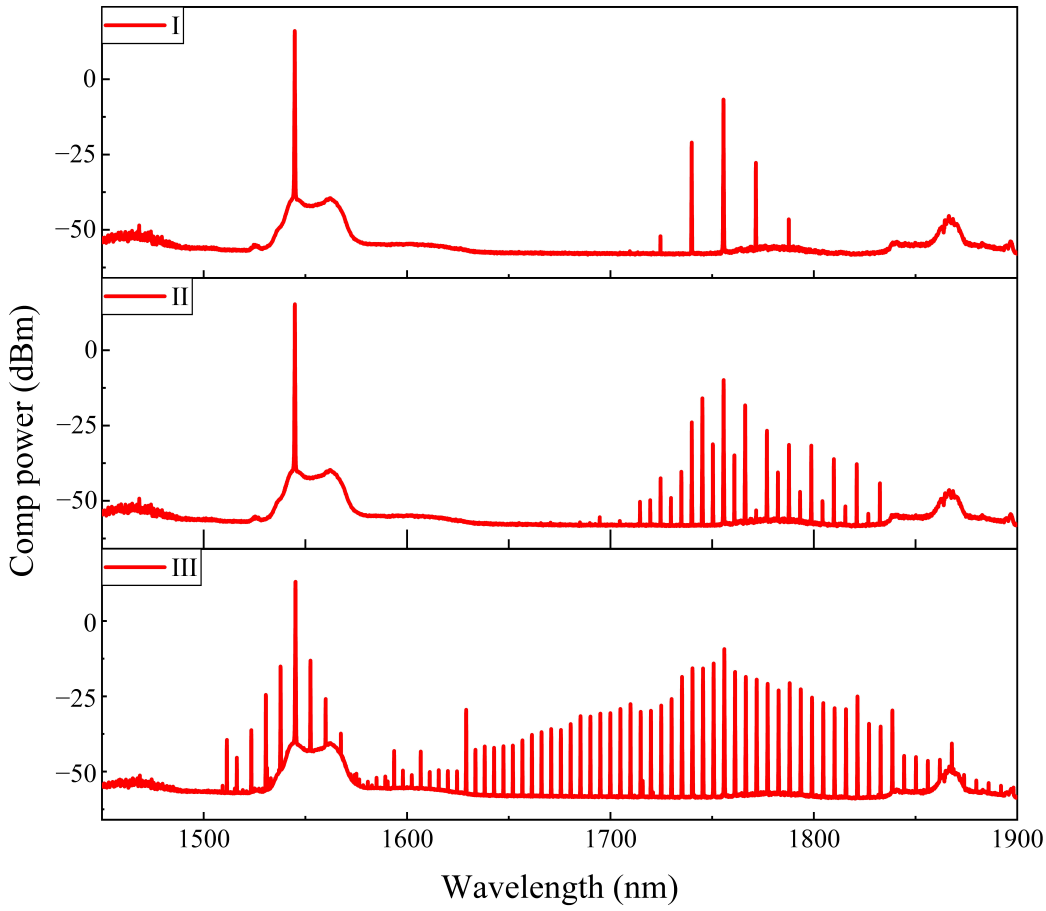

Fig. 3: Evolution of Raman comb and Kerr FWM comb. (I) SRS Stokes line appears at around 1775 nm with few sidebands. (II) Few Raman sidebands emerge. (III) Single FSR Raman comb coexists with multi-FSR (primary comb) Kerr comb around the pump wavelength.

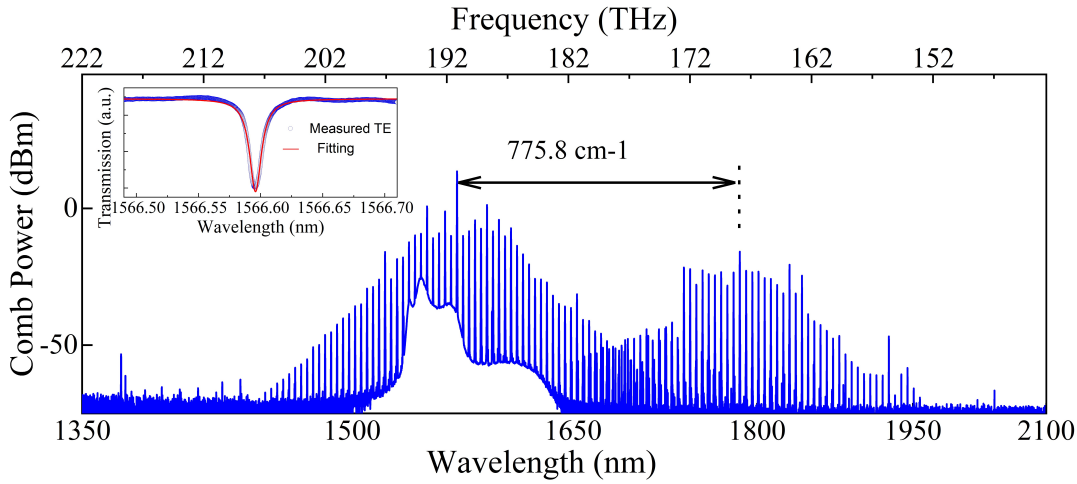

Fig. 4: Measured spectrum of Raman and Kerr comb in the wavelength range of 1450-1900 nm. The left inset is the zoomed-in image of the fitted pump transmission trace.

Summary

In summary, we have conducted an investigation into well-designed (anomalous dispersion) microresonators based on the 4H-SiCOI platform in the context of nonlinear photonics. Pumping the TE polarization modes, Raman-assisted comb and Kerr frequency combs via FWM are demonstrated. Strong

Raman lines (Stokes) are generated and this process is dominant over the FWM Kerr comb. Furthermore, our findings are significant for the continued exploration of on-chip Raman laser within the 4H-SiCOI platform and for various applications [27], including those in biological and spectroscopy.

References

[1] F. Tara and B. Esther: Comm. Phy. Vol. 2 (2019), p. 153

[2] Y. Geng, H. Zhou, X. Han, W. Cui, Q. Zhang, B. Liu, G. Deng, Q. Zhou and K. Qiu: Nat. Comm. Vol. 13 (2022), p. 1070

[3] J. Riemensberger, A. Lukashchuk, M. Kaprov, W. Weng, E. Lucas, J. Liu, and T. J. Kippenberg: Nature Vol. 581 (2020), p. 164-170

[4] D. T. Spencer, T. Drake, T. C. Briles, J. Stone, L. C. Sinclair, C. Fredrick, Q. Li, D. Westly, B. R. llic, A. Bluestone, N. Volet, T. komljenovic, L. Chang, S. Lee, D. Y. Oh, M. G. Suh, K. Y. Yang, M. H. P. Pfeiffer, T. J. Kippenberg, E. Norberg, L. Theogarajan, K. Vahala, N. R. Newbury, K. Srinivasan, J. E. Bowers, S. A. Diddams, and S. B. Papp: Nature Vol. 557 (2018), p. 81-85

[5] M. G. Suh, Q. F. Yang, X. Yi, K. J. Vahala: Science Vol. 354 (2016), p. 600-603

[6] P. Del'Haye, A. Schliesser, O. Arcizet, T. Wilken, R. Holzwarth and T. J. Kippenberg: Nature Vol. 450 (2007), p. 1214-1217

[7] A. G. Griffith, R. K.W. Lau, J. Cardenas, Y. Okawachi, A. Mohanty, R. Fain, Y. H. D. Lee, M. Yu, C. T. Phare, C. B. Poitras, A. L. Gaeta and M. Lipson: Nat. Comm. vol. 6 (2015), p. 6299

[8] J. S. Levy, A. Gondarenko, M. A. Foster, A. C. Turner-Foster, A. L. Gaeta and M. Lipson: Nat. Photon. vol. 4 (2010), p. 37-40

[9] H. Weng, A. A. Afridi, J. Li, M. McDermott, H. Tu, L. P. Barry, Q. Lu, W. Guo and J. F. Donegan: APL. Photonics vol. 7 (2022)

[10] H. Jung, C. Xiong, K. Y. Fong, X. Zhang, and H. X. Tang: Optics Lett. vol. 38 (2013), p. 2810-2813

[11] J. Liu, H. Weng, A. A. Afridi, J. Li, J. Dai, X. Ma, H. Long, Y. Zhang, Q. Lu, J. F. Donegan, and W. Guo: Optics Exp. vol. 28 (2020), p. 19270-19280

[12] H. Weng, J. Liu, A. A. Afridi, J. Li, J. Dai, X. Ma, Y. Zhang, Q. Lu, J. F. Donegan, and W. Guo: Photon. Research vol. 9 (2021), p. 1351-1357

[13] H. Yang, Q. F. Yang, J. Ling, R. Luo, H. Liang, M. Li, K. Vahala, and Q. Li: Optica vol. 6 (2019), p. 1138-1144

[14] L. Chang, W. H. Shu, Q. F. Yang, B. Shen, A. Boes, J. D. Peter, W. Jin, C. Xiang, S. Liu, G. Moille, S. P. Yu, X. Wang, K. Srinivasan, S. B. Papp, K. Vahala and J. E. Bowers: Nat. Comm. vol. 11 (2020), p. 1331

[15] X. Shi, W. Fan, A. Yi, X. Ou, K. Rottwitt and H. Ou in: CLEO Europe (2021), p. 1-1

[16] L. Cai, J. Li, R. Wang, and Q. Li: Photon. Research vol. 10 (2022), p. 870-876

[17] X. Shi, Y. Lu, D. Chaussende, K. Rottwitt and H. Ou: Materials vol. 16 (2023), p. 2343

[18] C. Wang, Z. Fang, A. Yi, B. Yang, Z. Wang, L. Zhou, C. Shen, Y. Zhou, R. Bao. and Z. Li: Light Sci. Appl. vol. 10 (2021), p. 139

[19] Th. Udhem, R. Holzwarth, and T. W. Hänsch: Nature vol. 416 (2002), p. 233-237

[20] M. A. Guidry, D. M. Lukin, K. Y. Yang, R. Trivedi and J. Vučković: Nature Photon. vol. 16 (2022), p. 52-58

[21] S. Fujii, and T. Tanabe: Nanophoton. vol. 9 (2020), p. 1087-1104

[22] A. A. Afridi, H. Weng, J. Li, J. Liu, M. McDermott, Q. Lu, W. Guo and J. F. Donegan: Optics Cont. vol. 1 (2022), p. 42-50

[23] H. Harima: Microelectronic Eng. vol. 83 (2006), p. 126-129

[24] G. Lin, and Y. K. Chembo: Optics Lett. vol. 41 (2016), p. 3718-3721

[25] Z. Gong, M. Li, X. Liu, Y. Xu, J. Lu, A. Bruch J. B. Surya, C. Zou and X. H. Tang: Physical Rev. Lett. vol. 125 (2020), p. 183901

[26] H. Weng, J. Liu, A. A. Afridi, J. Li, J. Dai, X. Ma, Y. Zhang, Q. Lu, J. F. Donegan and W. Guo: Optics Lett. vol. 46 (2021), p. 540-543

[27] H. Ou, X. Shi, Y. Lu, M. Kollmuss, J. Steiner, V. Tabouret, M. Syväjärvi, P. Wellmann and D. Chaussende: Materials vol. 16 (2023), p. 1014